Theoretical Studies on the Mechanism of the *Tropo*-Inversion of the BIPHEP-$RuCl_2$/DPEN Complex Using the ONIOM Method

Masahiro Yamanaka and Koichi Mikami*

Department of Applied Chemistry, Tokyo Institute of Technology, Tokyo 152-8552, Japan

Received March 21, 2002

The mechanism of *tropo*-inversion of the Ru(II) complex bearing a chirally flexible biphenylphosphine (BIPHEP) ligand has been studied by the B3LYP and the ONIOM(B3LYP:HF) methods. The relative energy difference between the favorable (*S*)/(*S*,*S*) and the less favorable (*R*)/(*S*,*S*) pairs of BIPHEP-$RuCl_2$/DPEN complexes is well comparable to the experimental results. The *tropo*-inversion of the (*S*)/(*S*,*S*) pair to the (*R*)/(*S*,*S*) pair is found to be achieved by solvent-assisted rotation around the biphenyl single bond and subsequent recoordination of phosphine to the Ru center. The sterically demanding phenyl groups attached to phosphorus atoms in the BIPHEP-$RuCl_2$ moiety prevented the internal rotation without dissociation of P−Ru coordination.

In asymmetric catalytic reactions, racemic catalysts inherently afford only racemic mixtures of chiral products.[1] Conversely, we reported a strategy for asymmetric catalysis where racemic catalysts bearing chirally flexible *tropos* ligands such as bis(phosphanyl)biphenyl (BIPHEP) were used.[2] Related strategies have recently been employed with varying degrees of enantioselectivity.[3] A chiral additive interacts with racemic but *tropos* ligands to define the chiral environment of the latter. In principle, a single diastereomeric catalyst formed after complexation with a chiral additive can achieve high enantioselectivity if the chiral additive acts as a chiral activator capable of selectively activating one of the enantiomers of the racemic catalysts. In our strategy, addition of a chiral activator can not only control the chirality of chirally flexible ligands through isomerization of *tropos* catalysts (*tropo*-inversion[4]) but also increase the catalytic activity (e.g., asymmetric activation[2a,5]) to produce high enentiomeric excess in the products (Scheme 1).

Scheme 1. Strategy Using the Chirally Flexible *Tropos* Catalysts

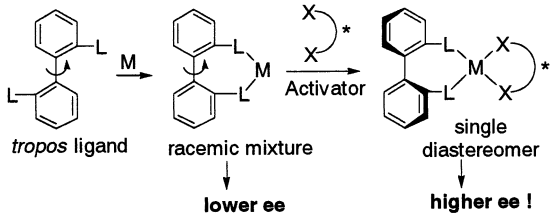

Scheme 2. Asymmetric Hydrogenation Using the Racemic XylBIPHEP-$RuCl_2$ Catalyst

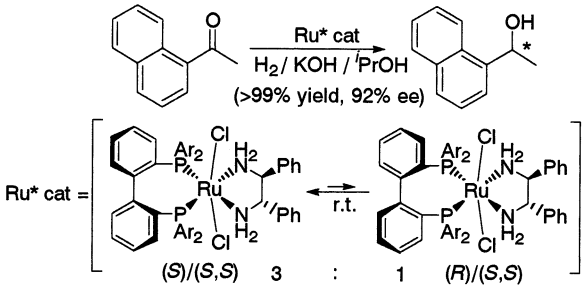

Upon addition of 1,2-diphenylethylenediamine (DPEN) as a chiral activator to the racemic XylBIPHEP-$RuCl_2$ (XylBIPHEP = 2,2′-[(3,5-dimethylphenyl)phosphanyl]-biphenyl), the diastereomeric catalyst can be formed to achieve high enantioselectivity in hydrogenation of ketones.[2c] The racemic BIPHEP-$RuCl_2$ and (*S*,*S*)-DPEN initially provide both diastereomers, (*S*)-XylBIPHEP-$RuCl_2$/(*S*,*S*)-DPEN and (*R*)-XylBIPHEP-$RuCl_2$/(*S*,*S*)-DPEN, in an equal amount, which eventually evolved in a 3:1 ratio (Scheme 2).

To design a chiral activator for complete control of the chirality of racemic but *tropos* catalysts, it is

* Corresponding author. E-mail: kmikami@o.cc.titech.ac.jp.

(1) (a) Noyori, R. *Asymmetric Catalysis in Organic Synthesis*; Wiley: New York, 1994. (b) Brunner, H.; Zettlmeier, W. *Handbook of Enantioselective Catalysis*; VCH: Weinheim, 1993. (c) *Catalytic Asymmetric Synthesis*; Ojima, I., Ed.; VCH: New York, 1993, 2000; Vols. I and II. (d) Kagan, H. B. *Comprehensive Organic Chemistry*; Pergamon: Oxford, 1992; Vol. 8.

(2) (a) Mikami, K.; Terada, M.; Korenaga, T.; Matsumoto, Y.; Ueki, M.; Angelaud, R. *Angew. Chem., Int. Ed.* **2000**, *39*, 3532−3556. (b) Mikami, K.; Aikawa, K.; Yusa, Y.; Jodry, J. J.; Yamanaka, M. *Synlett* **2002**, 1561−1578. (c) Mikami, K.; Korenaga, T.; Terada, M.; Ohkuma, T.; Pham, T.; Noyori, R. *Angew. Chem., Int. Ed.* **1999**, *38*, 495−497. (c) Ueki, M.; Matsumoto, Y.; Jodry, J. J.; Mikami, K. *Synlett* **2001**, 1889−1892. (d) Mikami, K.; Aikawa, K.; Yusa, Y.; Hatano, M. *Org. Lett.* **2002**, *4*, 91−94. (e) Mikami, K.; Aikawa, K.; Yusa, Y. *Org. Lett.* **2002**, *4*, 95−97. (f) Mikami, K.; Aikawa, K. *Org. Lett.* **2002**, *4*, 99−101.

(3) (a) Hashihayata, T.; Ito, Y.; Katsuki, T. *Synlett* **1996**, 1079−1081. (b) Hashihayata, T.; Ito, Y.; Katsuki, T. *Tetrahedron* **1997**, *53*, 9541−9552. (c) Pritchett, S.; Walsh, P. J. *J. Am. Chem. Soc.* **1998**, *120*, 6423−6424. (d) Miura, K.; Katsuki, T. *Synlett* **1999**, 783−785. (e) Ringwald, M.; Stürmer, R.; Brinzinger, H. H. *J. Am. Chem. Soc.* **1999**, *121*, 1524−1527. (f) Balsells, J.; Walsh, P. J. *J. Am. Chem. Soc.* **2000**, *122*, 1802−1803. (g) Balsells, J.; Betancort, J. M.; Walsch, P. J. *Angew. Chem., Int. Ed.* **2000**, *39*, 3428−3430. (h)White, P. S.; Gagne, M. R. *J. Am. Chem. Soc.* **2001**, *123*, 9478−9479.

(4) Oki, M. *Top. Stereochem.* **1983**, *14*, 1−76.

(5) Mikami, K.; Matsukawa, S. *Nature* **1997**, *385*, 613−615; *Enantiomer* **1996**, *1*, 69−73.

10.1021/om020215c CCC: $22.00
Publication on Web 11/22/2002

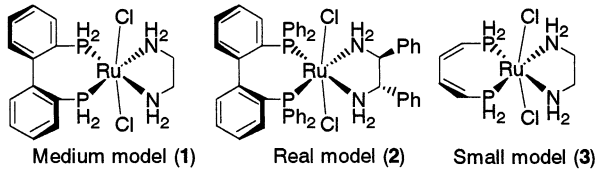

Figure 1. Chemical models of the BIPHEP-$RuCl_2$/DPEN complex.

Scheme 3. Three Possible Mechanisms of *Tropo*-Inversion of the BIPHEP-$RuCl_2$/DPEN Complex

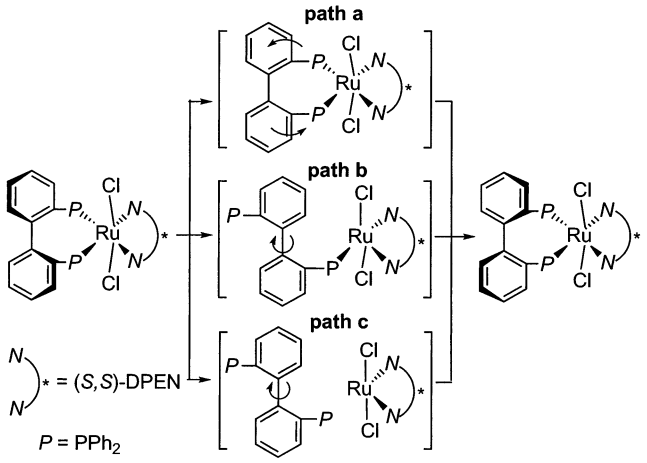

essential to understand the mechanism of the *tropo*-inversion. We herein describe theoretical studies on the mechanism of the *tropo*-inversion of the BIPHEP-$RuCl_2$/DPEN complex. Three possible mechanisms can be proposed for the *tropo*-inversion of the BIPHEP-$RuCl_2$/DPEN complex: (a) internal rotation between the biphenyl rings; (b) dissociation of only one P−Ru coordination and rotation back to the enantiomeric BIPHEP-$RuCl_2$ complex; (c) dissociation of two P−Ru coordinations (Scheme 3). To clarify the mechanism, we compared the activation barrier for internal rotation between biphenyl rings (path a) with dissociation of one P−Ru coordination and rotation (path b).

Chemical Models and Computational Methods

Two chemical models, **1** (medium model) and **2** (real model), were carried out by the B3LYP[6] and the ONIOM(B3LYP:HF) method,[7] respectively (Figure 1). All calculations were performed by the Gaussian 98 package.[8] In the medium model (**1**), H atoms were used instead of phenyl groups attached to phosphorus atoms as well as those in the DPEN moiety. The medium model **1** was optimized at the B3LYP level of calculation with the basis set denoted as 631SDD, consisting of Sttutgart's effective core potential[9] for Ru atoms and the 6-31G(d) basis set[10] for the rest. On the other hand, the real model (**2**) was optimized using the ONIOM method, which has been proven to be a powerful tool for the theoretical treatment of large molecular systems. The real system of the BIPHEP-$RuCl_2$/DPEN complex was divided into two layers, **2** and **3**, as shown in Figure 1.[11] The small model (**3**) with H atoms and a dienyl group instead of phenyl groups and a biphenyl group was treated at the higher-level method, B3LYP, with the 631SDD basis set. The full real model (**2**) including phenyl and biphenyl groups was treated at the lower-level method, Universal force field (UFF)[12] or HF, with the basis set denoted as 321LAN consisting of a LANL2DZ effective core potential[13] for Ru atoms and the 3-21G basis set[10] for the rest. Natural charges were calculated by the natural population analysis[14] at the B3LYP/631SDD level for optimized geometries. It was shown by the intrinsic reaction coordinate (IRC) analysis[15] followed by the geometry optimization that the sequence of the stationary points (*S*)/(*S*,*S*)-**1** → **TS1a** → (*R*)/(*S*,*S*)-**1** and (*S*)/(*S*,*S*)-**1** → **TS1b** is smoothly connected along the reaction coordinate.

Results and Discussion

The mechanism of the *tropo*-inversion of the BIPHEP-$RuCl_2$/DPEN complex was examined by using the two models **1** and **2**. The medium model **1** was first employed to study in detail the whole reaction pathway and solvent coordination effect on the Ru center. The real model **2** was treated only to estimate the steric effect of phenyl groups attached to phosphorus atoms. We have already reported no *tropo*-inversion through simultaneous dissociation of two P−Ru coordinations (path c) due to observing no ligand exchange between BIPHEP and BINAP by addition of BINAP.[16] We thus compared the activation barrier for internal rotation between biphenyl rings (path a) with dissociation of one P−Ru coordination and rotation (path b). Two possible transition states of *tropo*-invertion were employed on the basis of the two models, **1** and **2**.

Medium Model Study: *Tropo*-Inversion Mechanism. The *tropo*-invertion from (*S*)/(*S*,*S*)-**1** to (*R*)/(*S*,*S*)-**1** proceeds via two possible transition states, **TS1a** and **TS1b**. Two diastereomer, (*S*)/(*S*,*S*)-**1** and (*R*)/(*S*,*S*)-**1**, were fully optimized under C_2 symmetry at the B3LYP/631SDD level. The P−Ru and N−Ru lengths are the

(6) (a) Becke, A. D. *J. Chem. Phys.* **1993**, *98*, 5648−5652. (b) Lee, C.; Yang, W.; Parr, R. G. *Phys. Rev. B* **1988**, *37*, 785−789.

(7) (a) Maseras, F.; Morokuma, K. *J. Comput. Chem.* **1995**, *16*, 1170−1179. (b) Svensson, M.; Humbel, S.; Froese, R. D. J.; Matsubara, T.; Sieber, S.; Morokuma, K. *J. Phys. Chem.* **1996**, *100*, 19357−19363. (c) Dapprich, S.; Komaromi, I.; Byun, K. S.; Morokuma, K.; Frisch, M. J. *J. Mol. Struct. (THEOCHEM)* **1999**, *461*−*462*, 1−21. (d) Vreven, T.; Morokuma, K. *J. Comput. Chem.* **2000**, *21*, 1419−1432.

(8) Frisch, M. J.; Trucks, G. W.; Schlegel, H. B.; Scuseria, G. E.; Robb, M. A.; Cheeseman, J. R.; Zakrzewski, V. G.; Montgomery, J. A., Jr.; Stratmann, R. E.; Burant, J. C.; Dapprich, S.; Millam, J. M.; Daniels, A. D.; Kudin, K. N.; Strain, M. C.; Farkas, O.; Tomasi, J.; Barone, V.; Cossi, M.; Cammi, R.; Mennucci, B.; Pomelli, C.; Adamo, C.; Clifford, S.; Ochterski, J.; Petersson, G. A.; Ayala, P. Y.; Cui, Q.; Morokuma, K.; Salvador, P.; Dannenberg, J. J.; Malick, D. K.; Rabuck, A. D.; Raghavachari, K.; Foresman, J. B.; Cioslowski, J.; Ortiz, J. V.; Baboul, A. G.; Stefanov, B. B.; Liu, G.; Liashenko, A.; Piskorz, P.; Komaromi, I.; Gomperts, R.; Martin, R. L.; Fox, D. J.; Keith, T.; Al-Laham, M. A.; Peng, C. Y.; Nanayakkara, A.; Challacombe, M.; Gill, P. M. W.; Johnson, B.; Chen, W.; Wong, M. W.; Andres, J. L.; Gonzalez, C.; Head-Gordon, M.; Replogle, E. S.; Pople, J. A. *Gaussian 98*, Revision A.11; Gaussian, Inc.: Pittsburgh, PA, 2001.

(9) (a) Dolg, M.; Wedig, U.; Stoll, H.; Preuss, H. *J. Chem. Phys.* **1987**, *86*, 866−872. (b) Andrae, D.; Häussermann, U.; Dolg, M.; Stoll, H.; Preuss, H. *Theor. Chim. Acta* **1990**, *77*, 123−141.

(10) Hehre, W. J.; Radom, L.; Schleyer, P. v. R.; Pople, J. A. *Ab Initio Molecular Orbital Theory*; John Wiley: New York, 1986, and references therein.

(11) The SCF calculation failed to converge when the medium model **1** was used as a target model calculated at higher level in the ONIOM method.

(12) Rappé, A. K.; Casewit, C. J.; Colwell, K. S.; Goddard, W. A., III; Skiff, W. M. *J. Am. Chem. Soc.* **1992**, *114*, 10024−10035.

(13) (a) Wadt, W. R.; Hay, P. J. *J. Chem. Phys.* **1985**, *82*, 270−283. (b) Wadt, W. R.; Hay, P. J. *J. Chem. Phys.* **1985**, *82*, 99−310.

(14) Reed, A. E.; Weinstock, R. B.; Weinhold, F. *J. Chem. Pys.* **1985**, *83*, 735−746.

(15) (a) Fukui, K. *Acc. Chem. Res.* **1981**, *14*, 363−368. (b) Gonzalez, C.; Schlegel, H. B. *J. Chem. Phys.* **1989**, *90*, 2154−2161. (c) Gonzalez, C.; Schlegel, H. B. *J. Phys. Chem.* **1990**, *94*, 5523−5527.

(16) Korenaga, T.; Aikawa, K.; Terada, M.; Kawauchi, S.; Mikami, K. *Adv. Synth. Catal.* **2001**, *343*, 284−288.

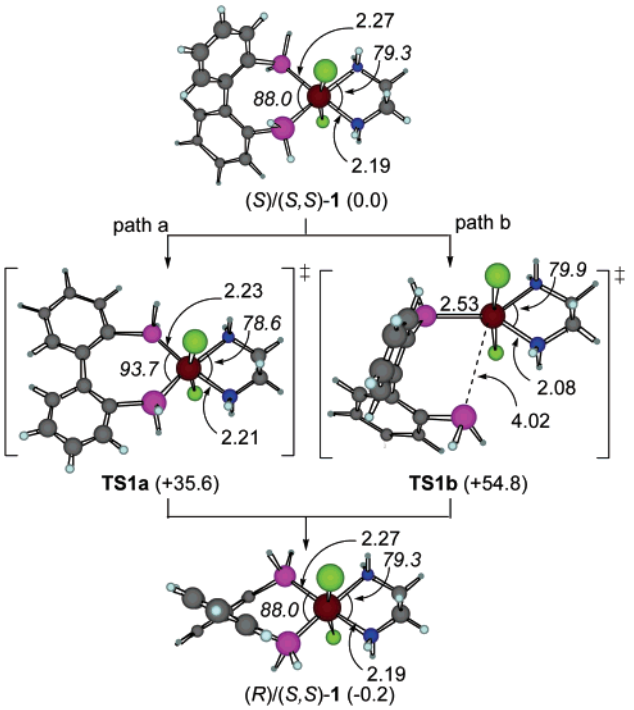

Figure 2. 3D structures and the relative energies (in parentheses) of (*S*)/(*S*,*S*)-**1**, (*R*)/(*S*,*S*)-**1**, **TS1a**, and **TS1b** at the B3LYP/631SDD level. Bond lengths and angles (*italic*) are in Å and deg, respectively. Color code: Ru = brown, P = purple, N = blue, Cl = green, C = gray, H = small blue spheres.

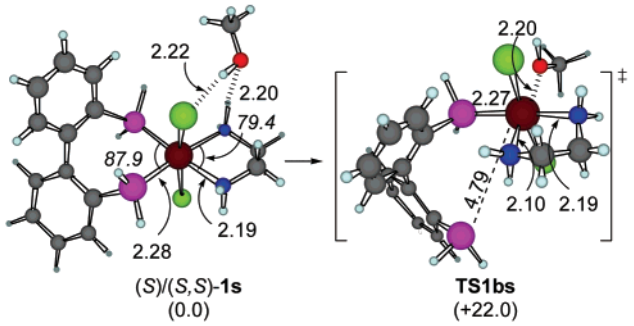

Figure 3. Solvated model of the P−Ru dissociation (path b). Bond lengths and angles (*italic*) are in Å and deg, respectively. Color code: Ru = brown, P = purple, N = blue, O = red, Cl = green, C = gray, H = small blue spheres.

same in both (*S*)/(*S*,*S*)-**1** and (*R*)/(*S*,*S*)-**1** as well as the P−Ru−P and N−Ru−N angles. The difference of energies between (*S*)/(*S*,*S*)-**1** and (*R*)/(*S*,*S*)-**1** is within 1.0 kcal/mol due to geometrical differences between two diastereomers, (*S*)/(*S*,*S*) and (*R*)/(*S*,*S*) forms, which are mainly found in the torsion ring composed of diphosphine and diamine (Figure 2). In the transition state of the internal rotation of biphenyl rings (path a; **TS1a**), the biphenyl rings were fixed on the same plane to optimize the other variables of the structure under C_2 symmetry. The transition state of the first dissociation of one P−Ru coordination before the rotation of biphenyl rings (path b; **TS1b**) was fully optimized under C_1 symmetry. As shown in Figure 3, **TS1b** is close to the trigonal bipyramidal structure since the diamine ligand coordination was distorted to push out one phosphorus atom.

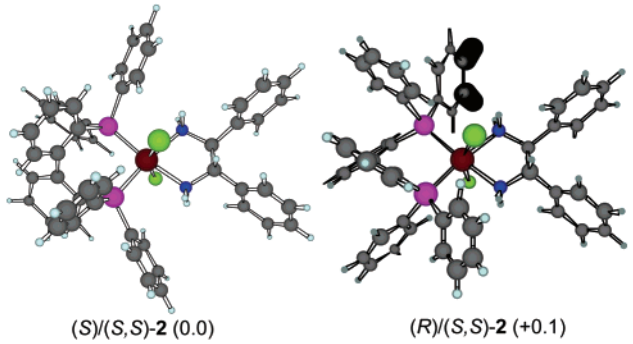

Figure 4. 3D structures and the relative energies (in parentheses) of (*S*)/(*S*,*S*)-**2** and (*R*)/(*S*,*S*)-**2** at the ONIOM-(B3LYP/631SDD:HF/321LAN) level. Color code: Ru = brown, P = purple, N = blue, Cl = green, C = gray, H = small blue spheres.

The activation energy of the internal rotation (path a: **TS1a**) is 36 kcal/mol. The 55 kcal/mol activation energy of the one P−Ru dissociation (path b: **TS1b**) is 19 kcal/mol larger than that of **TS1a**. However, the trigonal bipyramidal structure of **TS1b** indicates that **TS1b** can be stabilized by solvent coordination on the vacant site of the Ru center. Since the Ru center is saturated in **TS1a**, solvents cannot coordinate on the Ru center. Thus, only the solvent coordination effect in the dissociation of the P−Ru coordination (path b) was examined (Figure 3). We employed MeOH as a model solvent. The activation energy for the solvated transition state of **TS1bs** is much decreased to 22 kcal/mol, which is lower than that of internal rotation by 14 kcal/mol. Since the rotational barrier around the biphenyl single bond of BIPHEP is ca. 22 kcal/mol,[17] the rotation of the biphenyl rings after the first dissociation step can readily proceed at room temperature. The internal rotation pathway via **TS2a** is thus very unlikely to occur.

Real Model Study: Steric Effect on Phosphine of the BIPHEP Ligand. To estimate the steric effect of phenyl groups attached to phosphorus atoms, we next examined the real model **2**. The two-layered ONIOM-(B3LYP:HF) optimized structure of **2** is quite comparable to the B3LYP/631SDD optimized one, while the ONIOM(B3LYP:UFF) afforded a structure that has a long N−Ru distance and a narrow P−Ru−P angle (Figure 4, Table 1). It should be noted that the Cl−Ru−Cl angle was bent by the steric effect of phenyl groups attached to the phosphorus atoms (170.2° of **1** vs 160.9° and 158.9° of **2** at the B3LYP/631SDD and the ONIOM-(B3LYP:HF) levels). We thus concluded that the two-layered ONIOM calculation with the combination of the real model (**2**) at the B3LYP level and the small model (**3**) at the HF level can reproduce the structure in good agreement with that fully calculated at the B3LYP/631SDD level. At the present ONIOM(B3LYP:HF) level calculation, (*S*)/(*S*,*S*)-**2** is slightly more stable than (*R*)/(*S*,*S*)-**2**. The almost equal energies of (*S*)/(*S*,*S*)-**2** and (*R*)/(*S*,*S*)-**2** agree well with only a 3:1 diastereomeric ratio of the BIPHEP-RuCl$_2$/DPEN complex at room temperature.[2c]

The transition state of the internal rotation of biphenyl rings (path a; **TS2a**) was optimized under C_2

(17) Desponds, O.; Schlosser, M. *Tetrahedron Lett.* **1996**, *37*, 47−48.

Table 1. Distances and Angles in (*S*)/(*S,S*)-2 Optimized at the Various Calculation Levels

	Ru−P	Ru−N	Ru−Cl	P−Ru−P	N−Ru−N	Cl−Ru−Cl
B3LYP/631SDD	2.352	2.175	2.496	93.1	78.7	160.9
B3LYP/631SDD:HF/321LAN	2.343	2.173	2.503	92.8	78.9	158.9
B3LYP/631SDD:UFF	2.347	2.198	2.497	86.5	78.1	155.5

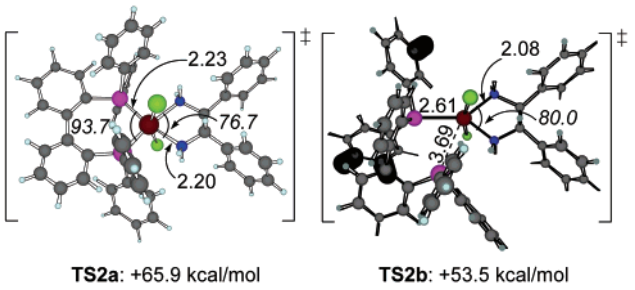

Figure 5. Transition structures and activation energies from the (*S*)/(*S,S*)-**2** pair for paths a and b at the ONIOM-(B3LYP/631SDD:HF/321LAN) level. Bond lengths and angles (*italic*) are in Å and deg, respectively. Color code: Ru = brown, P = purple, N = blue, Cl = green, C = gray, H = small blue spheres.

symmetry with the frozen coordinates of the biphenylphosphine-ruthenium moiety of **TS1a** except the Cl atoms and the phenyl groups attached to the phosphorus atoms. The transition state of the first dissociation of one P−Ru coordination before the rotation of the biphenyl rings (path b; **TS2b**) was fully optimized under C_1 symmetry. As shown in Figure 5, the structures of the real models, **TS2a** and **TS2b**, are very similar to those of the medium models, **TS1a** and **TS1b**. Since **TS2b** has a vacant site on the Ru center, **TS2b** can also be stabilized by solvent coordination as shown in the medium model of **TS1b**. While **TS2b** has almost the same activation energy of 54 kcal/mol as in **TS1b**,[18] the activation energy of **TS2a** is greatly increased up to 66 kcal/mol. The rotation around the biphenyl single bond of BIPHEP through the so-called cog-wheeling effect[19] depends only on the effective van der Waals radii. However, the large difference of the activation energy for **TS1a** and **TS2a** directly indicates that the internal rotation of biphenyl rings in the BIPHEP-$RuCl_2$ moiety was prevented by the sterically demanding phenyl groups attached to the phosphorus atoms.

Natural Population Analysis. As shown in Figure 6, the charge distributions of both **TS1a** and **TS2a** for the internal rotation pathway (path a) are very similar to those of **1** and **2**. In contrast, both **TS1b** and **TS2b** for the one P−Ru dissociation pathway (path b) are strongly polarized (dipole moment for **TS1a** 0.04 D, **TS2a** 0.02 D, **TS1b** 2.24 D, **TS1bs** 1.63 D, **TS2b** 2.67 D at the B3LYP/631SDD level). The polar transition states in series b was stabilized by coordination of the polar solvent such as ^{i}PrOH, which provides the polar reaction field, to accelerate dissociation of the P−Ru coordination. It is noted that dissociation of one P−Ru coordination makes the phosphorus atoms more negative and the Ru atom more positive. The larger activation energy of **TS1b** is originated from the strong polarization by larger charge transfer in **TS1b**. However, solvent (e.g., MeOH) coordination on the unsaturated Ru center much eased changes of the charge on the coordinated P atom and one N atom to decrease the activation barrier for path b. Thus, *tropo*-inversion of the BIPHEP-$RuCl_2$/DPEN complex readily proceeds in the polar solvent (e.g., ^{i}PrOH) to afford preferentially the favored (*S*)/(*S,S*) form, in agreement with the experimental results.[2c]

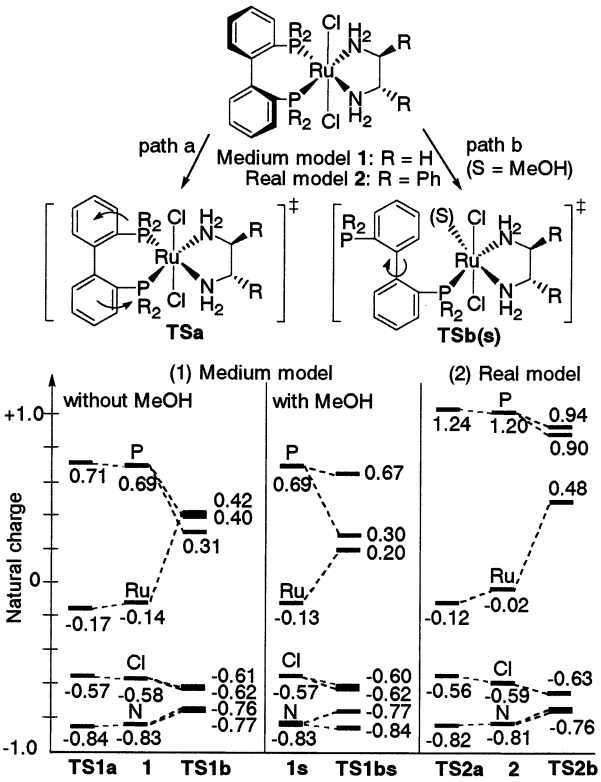

Figure 6. Natural population analysis of Ru, P, N, and Cl atoms in paths a and b for the medium model (**1**) and the real model (**2**).

Conclusion

We concluded that the *tropo*-inversion of the BIPHEP-$RuCl_2$/DPEN complex consists in the solvent-assisted rotation around the biphenyl single bond through the cog-wheeling effect and subsequent recoordination of phosphine to the Ru center, leading to the favorable diastereomer. The solvent coordination on the Ru center decreases the activation energy to assist the *tropo*-inversion via dissociation of one P−Ru coordination and rotation (path b). In contrast, there is no assistance of solvation in the internal rotation (path a) because of the nonpolar and saturated transition state. Furthermore, the sterically demanding phenyl groups on the phosphorus atoms prevent the internal rotation. The mechanism of the *tropo*-inversion described herein can be widely applied to transition metal complexes with BIPHEP ligands.

(18) As shown in the medium model **TS1bs**, solvent coordination on the Ru center in the real model **TS2b** should decrease the activation energy.

(19) (a) Bott, G.; Field, L. D.; Sternhell, S. *J. Am. Chem. Soc.* **1980**, *102*, 5618−5626. (b) Rousel, C.; Liden, A.; Chanon, M.; Metzger, J.; Sandstrom, J. *J. Am. Chem. Soc.* **1976**, *98*, 2847−2852. (c) Nilsson, B.; Martinson, P.; Olsson, K.; Carter, R. E. *J. Am. Chem. Soc.* **1974**, *96*, 3190−3197.

Acknowledgment. A generous allotment of computational time from the Institute for Molecular Science, Okazaki, Japan, and the Global Scientific Information and Computing Center, Tokyo Institute of Technology, is gratefully acknowledged.

Supporting Information Available: Tables giving geometries of the representative stationary points. This material is available free of charge via the Internet at http://pubs.acs.org.

OM020215C